RESEARCH ARTICLE

Estimation of Sensible and Latent Heat Fluxes of an Isolated Tree in Japanese Summer

Takashi Asawa[1] · Kunihiko Fujiwara[2]

Abstract

Considering that the characteristics of the heat balance between an isolated tree and the urban atmosphere have not yet been sufficiently clarified, we quantify both the sensible heat flux (H_T) and latent heat flux (lE_T) to and from an isolated *Z. Serrata* in the Japanese summer. To estimate the whole-tree transpiration rate (E_T) and lE_T values, we apply a previously developed method using a weighing lysimeter. To estimate the boundary-layer heat conductance (g_{hT}) of the total leaf area of the tree crown and the sensible heat flux (H_T), we apply a scaling-up approach using the heat-balance two-state (HB-TS) method, which previously only targeted single leaves, to the tree crown. Two sample trees with similar crown shape and total leaf area are selected for the HB-TS method but under different irrigation conditions, and g_{hT} is estimated. The E_T values of the tree change three times during the dry-down experiment (during which time irrigation was halted). We also compare H_T and lE_T values between two different days under different irrigation and soil–water conditions. The most important result from this comparison is that the tendencies of H_T and lE_T were reversed on these days, and the Bowen ratio ($\beta = H_T/lE_T$) dramatically varies between 0.29 and 2.2. These results indicate that the Bowen ratio of isolated trees at urban sites can vary between the previously reported values for forest sites and those for artificial urban sites within a short period, owing to urban-unique conditions (e.g., limited water supply and rooting space, and artificial sealing).

Keywords Boundary-layer heat conductance · Latent heat flux · Sensible heat flux · Whole-tree transpiration · Urban tree

1 Introduction

Transpiration is a physiological function of trees that has a cooling effect on the urban thermal environment. Transpiration from a leaf surface is described as the movement of

✉ Takashi Asawa
  asawa.t.aa@m.titech.ac.jp

[1] Department of Architecture and Building Engineering, Tokyo Institute of Technology, Yokohama, Kanagawa 226-8502, Japan

[2] Takenaka Research and Development Institute, Inzai, Chiba 270-1395, Japan

water vapour through stomata driven by the water potential difference between the leaf and atmosphere. Transpiration releases latent heat from the leaf surface, cooling both the leaf and the atmosphere. The transpiration rate (E) and latent heat flux (lE), where l is the latent heat of vaporization, of trees have typically been estimated using the porometer method (Leverenz et al. 1982; DeRocher et al. 1995), the sap-flow method (Swanson and Whitfield 1981; Granier 1987), and the lysimeter method (Edwards 1986; Lorite et al. 2012). Whole-tree transpiration can be accurately measured using weighing lysimeters if other factors involved in the water balance can be controlled or measured, and wind noise can be eliminated in the outdoor environment. Asawa et al. (2012, 2014a) developed a novel method to quantitatively measure the whole-tree transpiration rate (E_T) of a container-grown tree with a height of several metres using a weighing lysimeter. Asawa et al. (2017) quantified E_T for a *Z. serrata* tree, which had reached a height of 6.4 m over 3 years, by applying a data-quality control protocol for the long-term measurement of weight change to remove wind noise and other error factors. Urban trees tend to readily close stomata to decrease transpiration because of drought stress caused by significant vapour-pressure deficit, limited water supply and root space, and significant soil compaction (e.g., Kjelgren and Clark 1993; Cregg 1995; McCarthy and Pataki 2010; Osone et al. 2014; Kagotani et al. 2015). The container-grown conditions of Asawa et al. (2017) were set under the assumption that the root space for urban trees is limited by both shallow soil and pavements. Therefore, the effects of these urban-unique conditions on E_T values were effectively analyzed using the weighing-lysimeter method.

To reveal the thermal effect that the tree crown has on the surrounding atmosphere on a quantitative basis, it is necessary to quantify the sensible heat flux (H_T) for the total leaf area as well as the latent heat flux (lE_T). In the present study, H_T and lE_T are defined over the total leaf area (W m^{-2}) of an isolated tree. Net radiation (R_n, per leaf area) is converted into sensible and latent heat on the foliage of the crown; thus, to understand the effects on the urban thermal environment, it is insufficient to only estimate lE_T. Sensible heat transfer warms the surrounding atmosphere; consequently, the thermal effects on an urban environment largely depend on whether the heat flux from trees is mainly composed of sensible heat or latent heat. There is abundant research estimating H and lE over forests and vegetative land surfaces (see Sect. 2.1). To determine H and lE for such land cover, consideration of the horizontal distribution of heat fluxes is unnecessary except at the edges of such an environment, and one-dimensional heat and water exchange can be assumed between soil, plant, and atmosphere. However, difficulties arise when estimating H_T for the total leaf area of an individual tree, as described in the following: (a) A tree crown has a complex three-dimensional geometry, and its leaf area is distributed over the entire three-dimensional space within the crown. The three-dimensional distribution of the leaves affects the total amount of solar radiation received by the crown, and the radiative exchange within the crown and with its surroundings (Law et al. 2001; Yang and Friedl 2003; Parker et al. 2004); (b) Isolated trees, such as those in a street or garden, are often exposed to a greater advection of air than those in a forest. These effects produce an increase in evapotranspiration in urban areas, which is termed the oasis or leading-edge effect (Oke 1987; Kanda 2007; Hagishima et al. 2007); (c) Tree canopies are not the only source of heat and moisture. The forest floor is a source too (Roberts 1983; Schaap and Bouten 1997; Baldocchi et al. 2000), implying that separating the different components of the heat flux (e.g., transpiration or evaporation from wet ground) from the observations is difficult. Owing to such difficulties, the characteristics of H_T for isolated trees have not yet been sufficiently clarified.

Because H_T cannot be measured directly, it needs to be estimated. Focusing on the heat and water balance of individual leaves, scalar transfer (e.g., heat and mass) between the leaf and the surrounding atmosphere is driven by scalar density differences (e.g., temperature

and mass density difference) and is dominated by the leaf boundary-layer conductance (g_a). For transpiration, the stomatal conductance (g_s) is also a dominant factor. So far, theoretical examination and experiments to discern g_a have been made to understand both the absorption efficiency of carbon dioxide and the water-use efficiency for production by plants undergoing photosynthesis (Chen 2003; Shibuya et al. 2006). The boundary-layer heat conductance (g_h) is responsible for sensible heat transfer, and is dominated by the flow around the leaf surface as well as the leaf geometry and size (Hasebe 1984). In general, formulating g_h using a dimensionless number (e.g., the Nusselt number) for an outdoor environment in heat transfer theory is difficult (Hasebe 1984), because the leaves and branches sway freely in natural flow and are affected by complex turbulence (Schuepp 1972; Schuepp 1980). In addition, tree crowns are composed of foliage, the aggregate of individual leaves, and do not have a flat and large surface as with the wall of a building or the ground. Therefore, the g_h value of foliage covers the conductance between the collection of leaves and the surrounding atmosphere. A novel study by Asawa et al. (2016) estimated g_h for the total leaf area (g_{hT}) of *Z. Serrata* in an outdoor environment by using the heat-balance two-state (HB-TS) method, based on the aforementioned weighing-lysimeter method. The parameter g_{hT} is defined as the convective heat transfer coefficient ($W\,m^{-2}\,K^{-1}$) between a tree crown and the ambient air at a reference position, which is determined based on the total leaf area of the tree. The reference position is set at the outside of the tree crown where the aerodynamic effect of the tree can be neglected. The difference between g_h and g_{hT} arises from the difference in the method to measure heat transport, i.e., the former is based on a measurement of a single leaf, whereas the latter is based on the estimation of the total amount of heat transport between an isolated tree and the ambient air, divided by the total leaf area. It is clear that the latter is more difficult to determine than the former, as mentioned above.

In the present study, we identify the H_T values of *Z. Serrata* in an outdoor environment in summer by using the HB-TS method and quantitatively compare this with the lE_T values. The ratio of H_T and lE_T, the Bowen ratio, should change with the soil–water content; thus, the soil–water content is considered in the estimation and comparison process. The questions addressed are as follows: (a) How can the HB-TS method be applied to the estimation of the H_T value of an isolated tree? (b) What is the balance between the H_T and lE_T values under adequate irrigation in urban conditions? (c) How does the balance change under drought conditions? The data acquired to resolve these questions will inform our understanding of the cooling effect from urban trees and facilitate the investigation of appropriate irrigation control for isolated trees in an urban environment. These data will also be applied to the validation and parametrization of energy balance models for urban trees in microclimate simulations (Bruse and Fleer 1998; Asawa et al. 2008; Chen et al. 2011).

2 Literature Review

2.1 Methods Based on Remote Sensing

The eddy-covariance method is one of the most widely applied methods for measuring H and lE over forests, tree canopies, and vegetative surfaces (Anderson et al. 1984; Verma et al. 1986). Methods based on remote sensing have also been applied for the estimation of H and lE over these surfaces (Kalma et al. 2008), because the radiometric surface temperature is closely related to H (Lhomme et al. 1992; Lhomme et al. 1994; Zhan et al. 1996); it is also regarded as the primary parameter in estimating lE (Blad and Rosenberg 1976;

Choudhury et al. 1986; Miglietta et al. 2009). Radiometric surface temperatures have been obtained from satellite remote sensing for regional-scale areas (Sucksdorff and Ottle 1990; Mecikalski et al. 1999), airborne remote sensing for medium-scale areas (Kustas et al. 1989; Norman et al. 1995), and ground-based measurements for microscale areas (Vining and Blad 1992; Jones et al. 2018). In addition, energy balance models have been applied to remotely-sensed radiometric temperature data to estimate energy fluxes (sensible and latent heat fluxes) (Timmermans et al. 2007; Kalma et al. 2008). The two-source energy balance (TSEB) model (Cammalleri et al. 2012; Kustas et al. 2012; Colaizzi et al. 2012) and the surface energy balance algorithm for land (SEBAL) model (Bastiaanssen 2000; Paul et al. 2013; Tang et al. 2013) also have been frequently used in recent years. The primary target of all these methods is the calculation of one-dimensional fluxes and energy balances for target sites, including both homogeneous and heterogeneous land cover; however, this is not suitable for flux estimations of three-dimensional total leaf area for a tree crown of an isolated tree. This is because three-dimensional factors, including radiation and airflow, affect the energy balance of the tree crown. However, it has been suggested that remotely-sensed radiometric surface temperature has a high potential for representing H_T from the tree crown. In addition, the difficulties and limitations for flux estimations of the tree crown are not derived from the observation of the radiometric surface temperatures of the foliage (see Sect. 3.5) but from one-dimensional assumptions used in the estimation process.

2.2 Heat-Balance Method

There have been many studies showing the fundamental effects of leaf size and surrounding airflow on g_a based on dimensionless-number heat transfer theory (e.g., the Nusselt number, Balding and Cunningham 1976) that examine the detailed effects of turbulence (Schuepp 1972) and leaf flutter on g_a (Schuepp 1980). In particular, several studies suggest that g_a is increased by turbulence and leaf flutter in a natural environment because the leaf boundary layer becomes thinner owing to these effects (Schuepp 1980). This indicates the importance of the estimation of g_a in the natural environment, specifically outdoor spaces.

To measure g_a experimentally, several methods have been proposed for both real and artificial leaves (e.g., Defraeye et al. 2013). The representative methods are the water-loss technique for mass transfer and the heat-balance method for heat transfer. For the water-loss technique, an artificial leaf is wetted and weighed before and after the experiment, and the convective mass transfer coefficient is estimated from the water loss and vapour-pressure deficit on the leaf surface. The water-loss technique has also been applied to both artificial and small potted plants by measuring the total weight after wetting the leaves (Landsberg and Powell 1973).

For the heat-balance method, the g_h value of a leaf is estimated from the residual leaf heat balance by measuring R_n, E, and the temperature difference between the leaf surface and surrounding atmosphere (Kumar and Barthakur 1971; Parlange and Waggoner 1972; Martin et al. 1999). This method can be applied to both real and artificial leaves. For use on artificial leaves, the leaf is often heated artificially using a heater, thereby introducing an additional term (the heating term) to the leaf heat balance (Parkhurst et al. 1968; Murphy and Knoerr 1977). The HB-TS method, another type of heat-balance method, estimates g_h by setting two states for a pair of leaves, usually with and without transpiration. This method can eliminate heat-flow factors that are difficult to measure in the field, such as absorbed radiation, by applying simultaneous heat-balance equations for two states. For example, the transpiration of one leaf is suppressed by coating the leaf surface with Vaseline (Thrope and

Butler 1977) or by using anti-transpirants on the plants (Kitano et al. 1995), which close the stomata physiologically. These methods are considered to be valid under the condition that radiation absorbed is equivalent for the two leaves. The heat balances of leaves (both sides) with and without transpiration are given by

$$aS_i + \varepsilon L_i = lE + 2g_h(T_{l1} - T_a) + 2\sigma\varepsilon T_{l1}^4, \tag{1}$$

$$aS_i + \varepsilon L_i = 2g_h(T_{l2} - T_a) + 2\sigma\varepsilon T_{l2}^4. \tag{2}$$

By combining these equations simultaneously, g_h is given by

$$g_h = \frac{0.5lE - \sigma\varepsilon\left(T_{l2}^4 - T_{l1}^4\right)}{(T_{l2} - T_{l1})}. \tag{3}$$

By using the g_h value, the sensible heat fluxes from the leaves are then given by

$$H_1 = 2g_h(T_{l1} - T_a), \tag{4}$$

$$H_2 = 2g_h(T_{l2} - T_a), \tag{5}$$

where a is the absorptance for shortwave radiation of a leaf, S_i is incoming shortwave radiation, ε is emissivity, L_i is incoming longwave radiation, g_h is boundary-layer heat conductance (W m^{-2} K^{-1}), T_l is leaf temperature, T_a is the air temperature, σ is the Stefan–Boltzmann constant ($= 5.67 \times 10^{-8}$ W m^{-2} K^{-4}), and subscripts 1 and 2 refer to leaf 1 with transpiration and leaf 2 without transpiration, respectively.

As shown by Eq. 3, it is necessary for there to be a large temperature difference between the two leaves used in the HB-TS method. Because there is much research concerning the detection of the degree of water stress in plants by observing leaf temperature (T_l) (Tanner 1963; Jackson et al. 1981; Hatfield 1983), differences in E and T_l can be considered to be appropriate indices for the HB-TS method (Jones 2004; Blonquist Jr. et al. 2009). The HB-TS method has also been applied to artificial leaves; in this case one leaf was heated by a heater, and therefore, the differences in T_l were artificially set instead of occurring naturally via transpiration (Brenner and Jarvis 1995). Both the heat-balance method and the HB-TS method are applied to the estimation of g_h on walls under outdoor solar radiation and natural wind (the heat-balance method: Hagishima and Tanimoto 2003; Clear et al. 2003; the HB-TS method: Ito et al. 1972; Sharples 1984; Loveday and Taki 1996); thus, the application range for these methods is very wide. In general, an increase in the number of the variables to be measured leads to the accumulation of errors of measurement and estimation in the final results. However, the HB-TS method only requires the temperature differences for the two states of the leaves and E (or heating flux from a heater) as variables to be measured, if the absorbed radiation is assumed to be equivalent.

For both methods, most research targets an individual leaf, except when using small plants. Kitano et al. (1995) estimated the averaged g_a value for an entire individual plant (e.g., cucumber or lettuce) using an anti-transpirant (abscisic acid) and by weighing the plant under the two states (before and after applying the abscisic acid). Another novel trial by Asawa et al. (2016) estimated g_{hT} for the total leaf area of an isolated tree by applying the HB-TS method. In the study, E_T was measured using the weighing-lysimeter method (Asawa et al. 2017). The present study is implemented based on the methods of these two studies, targeting a real-sized tree.

3 Materials and Methods

3.1 Theoretical Examination

Considering the above-mentioned literature review and discussion, the important factors for estimating g_{hT} and H_T are as follows: (1) estimations of g_{hT} and H_T should include the movement of branches and leaf-flutter under natural wind conditions. (2) The HB-TS method is effective in reducing errors in the accumulation and propagation of measurements and estimations. (3) The difference in E_T and T_l between the two states is an effective parameter for estimation. (4) Changes to E_T cause clear changes in T_l. (5) The E_T and lE_T values of an isolated tree are measurable by using weighing lysimeters. (6) The radiometric surface temperature of a tree crown (T_r) has a high potential in representing T_l and H_T. (7) To minimize instrumental error (systematic error), the amount of equipment used for measurements and the number of variables measured should be minimized. As suggested, we apply the HB-TS method and the weighing-lysimeter method to the isolated tree and estimate H_T and lE_T for the two states with different T_l and E_T values. The estimation of total leaf area is also important in the method; thus, we apply a terrestrial-laser scanning system for the accurate estimation of the total leaf area of an isolated tree (Asawa et al. 2014b).

3.2 Plant Materials and Study Site

The sample tree was a 13-year-old *Z. serrata,* this being the third most popular street tree species in Japan (NILIM 2014), with a short trunk and long, upward-spreading stems covered with plentiful leaves. The shape of the tree implies that leaves and branches generally sway in natural wind; thus, the g_{hT} values are considered to be greater than for most urban trees. To apply the HB-TS method to the tree crowns, we selected two *Z. serrata* with similar features as sample plants (Fig. 1). The selection process was as follows: we prepared seven *Z. serrata* in the experimental field. All were produced by grafting in the same field on the same day in 1997. All were of almost the same height and were transplanted into large containers at the same time (February 2010). From these seven trees, we carefully selected two sample trees for measurement, which had similar crown shapes and leaf areas. The heights and trunk diameters in 2010 were 6.4 m and 0.11 m for tree A, and 6.3 m and 0.10 m for tree A′, respectively.

We measured the leaf areas of the two trees using a terrestrial-laser scanning system (VZ-400, RIEGL, Horn, Austria) in the summer of 2010. We then applied the voxel-based canopy profiling method to the laser-scanned data for the estimation of the total leaf areas (Hosoi and Omasa 2006; Oshio et al. 2015). In a previous study (Asawa et al. 2014b), we validated the method by comparison with the stratified clipping method and confirmed that this method estimates the total leaf area with an accuracy of 6% for *Z. serrata*. On 3 September, 2010, one-sided total leaf areas were found to be 13.2 m^2 for tree A and 11.9 m^2 for tree A′, respectively. The difference in the leaf area was 10%, which presumably results in a 10% error in the estimation of H_T using Eq. 10 (see Sect. 3.3). The *Z. serrata* trees were planted in large containers with an area of 1 m^2 and a depth of 0.6 m. The box volume was determined based on the rooting space of a general street tree (MLIT Japan 2005). The root-zone depth was 0.5 m, and the soil was composed of Kanto loam (70%), perlite (20%), and leaf mould (10%). Tree A had adequate transpiration under full irrigation (except for several days because of dry-down experiments). In contrast, we regarded tree A′ as a reference tree for the HB-TS
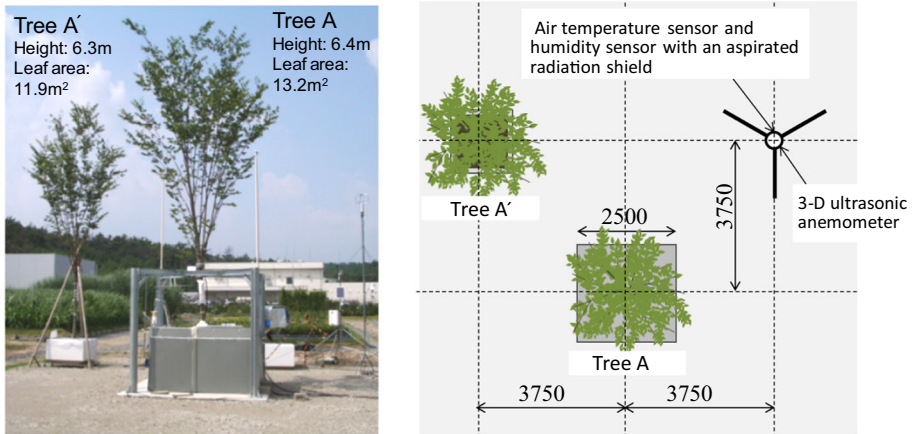
Fig. 1 Layout and information for tree A and tree A′

method; this tree had the least transpiration because of the cessation of irrigation for several successive days. Therefore, tree A′ suffered from drought stress and closed stomata on these days.

The study site chosen was an experimental field with an open area of 8800 m² in the city of Miyoshi, Aichi Prefecture, Japan (35° 8′ N, 137° 6′ E). There were no obstacles within 40 m of the sample trees, except several container-grown trees of 5-m height. Distances between these trees were > 4 m; thus, they were exposed to solar radiation and airflow. This may be regarded as an isolated condition for these sample trees.

3.3 Estimation of Boundary-Layer Heat Conductance (g_{hT}) and Sensible Heat Flux (H_T) of the Total Leaf Area

Asawa et al. (2016) estimated the averaged g_{hT} value of the total leaf area of the isolated tree. The present study deals with g_{hT} in the same way, using an estimation of H_T. To express H and lE for tree canopies, g_a and g_h are scaled up from single leaves to tree canopies (Campbell and Norman 1998; Blonquist Jr et al. 2009). If the transpiration rate of the tree canopies (E_c) can be estimated, then the latent heat flux from tree canopies is expressed as lE_c. The sensible heat flux from tree canopies (H_c) is expressed as

$$H_c = g_{hc}(T_c - T_a), \tag{6}$$

where T_c is canopy temperature and g_{hc} is the boundary-layer heat conductance of the tree canopy (W m⁻² K⁻¹). Equation 6 treats the canopy as a "big-leaf" for estimating g_{hc} (Baldocchi et al. 1991), while T_c is the effective temperature of the canopy for H_c that satisfies Eq. 6 (Kustas and Norman 2000). Previously, T_c was mostly estimated from the measurement of surface radiometric temperature (T_r), and the difference between T_c and T_r was used (Norman et al. 1995; Blonquist Jr. et al. 2009). The difference between T_c and T_r increases when the infrared radiometer used to measure T_c also measures the underlying soil through the foliage gaps. In addition, an appropriate correction for surface emissivity is required for accurate surface temperature measurements for the tree canopy, if T_r is significantly different from the behind temperature (i.e., radiant temperature from the direction of the reflection, e.g., the sky temperature behind the thermal infrared camera). In addition, Eq. 6 assumes
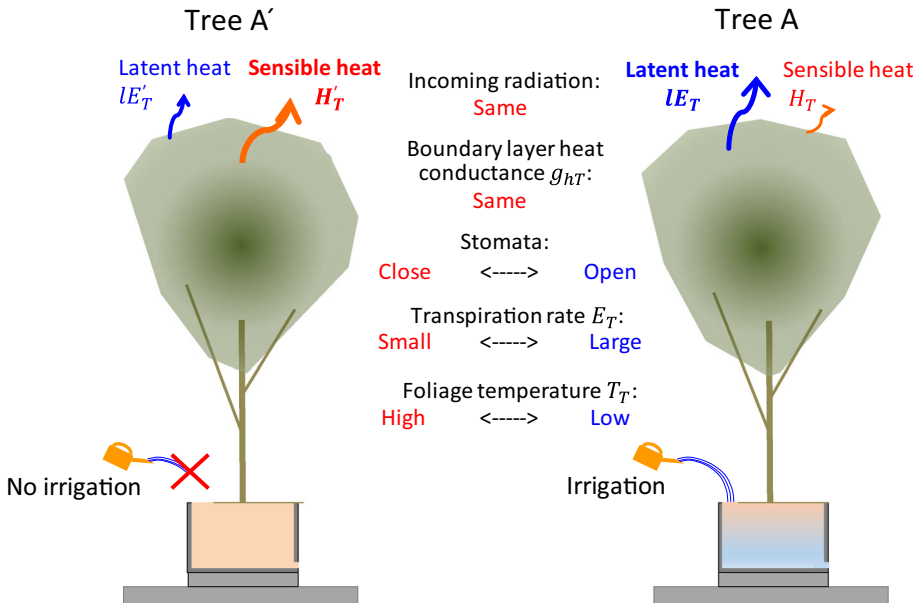
Fig. 2 Image of the HB-TS method for the total leaf areas of isolated trees

that the measured values of T_c are representative of the entire canopy, applying the same weighting from all the individual leaves. The radiometric temperature is a composite value weighted from all the elements within the radiometer field of view. The calculated value of g_{hc} is valid for the canopy within the field of view and is representative of the entire canopy or field only when the canopy is homogeneous (Blonquist Jr. et al. 2009). These points are also discussed in Sect. 3.5 for the measurement of T_r for a tree crown. The present study applies the same scaling-up approach for the estimation of the g_{hT} and H_T values of the total leaf area of an isolated tree, using T_r as the representative of the foliage temperature (T_T). However, both the estimation method and the procedure are new and relatively untested.

To estimate the g_{hT} and H_T values of the total leaf area, the HB-TS method is applied to the heat balance of two individual tree crowns (tree A and tree A′) with different E_T values in the same outdoor environment (Fig. 2). The difference in E_T between two trees is made by controlling irrigation conditions. Here, the net heat balance is estimated for the tree crown, and the fluxes (radiation flux, H_T and lE_T) are estimated per leaf area of the foliage. The primary requirement of applying the HB-TS method to the total leaf areas of isolated trees is that tree A and tree A′ are the same species of tree, same age, same size, and have the same leaf area. If two trees are in the same environment and the crown shape and leaf areas are very similar, the incoming radiation fluxes and the g_{hT} values can be assumed to be equivalent.

Therefore, the heat balances of tree A and tree A′, based on that of single leaves (Eqs. 1 and 2), are given by

$$a_T S_{iT} + \varepsilon_T L_{iT} = lE_T + 2g_{hT}(T_T - T_a) + 2\sigma\varepsilon_T T_T^4, \tag{7}$$

$$a_T S_{iT} + \varepsilon_T L_{iT} = lE_T' + 2g_{hT}\left(T_T' - T_a\right) + 2\sigma\varepsilon_T T_T'^4, \tag{8}$$

where subscript T indicates the average value over the total leaf area, and T_a is air temperature at a reference position with negligible aerodynamic effect of the tree.

When there is large difference in E_T values between tree A and tree A′, foliage temperature (T_T) should also differ between them. Therefore, if values for E_T and T_T are identified for these trees, the relation for g_{hT} can be obtained from the simultaneous calculation of Eqs. 7 and 8,

$$g_{hT} = \frac{0.5\left(lE_T^{'} - lE_T\right) - \sigma\varepsilon\left(T_T^{'4} - T_T^4\right)}{\left(T_T^{'} - T_T\right)}.$$ (9)

This equation is also equivalent to that for single leaves as shown by Eq. 3. Although it is quite difficult to ensure perfect equality in the crown shape and total leaf area of the two trees, the difference in T_T is the primary factor for the estimation of g_{hT}. Therefore, small differences in geometric factors (shape and leaf area) do not produce a significant error in the result for g_{hT}.

The H_T value can be estimated from the g_{hT} and T_T values via

$$H_T = 2g_{hT}(T_T - T_a),$$ (10)

where H_T is the sensible heat flux per leaf area (considering both sides). Here, T_T is obtained from the remotely-sensed T_r value as explained in Sect. 3.5. If needed, the H_T value can be converted into that based on the ground area by multiplying by the leaf area index ($LAI =$ total leaf area of one side divided by the vertical projected area of the crown). Here, the LAI value of the target tree (tree A) is 2.4.

3.4 Estimation of Latent Heat Flux of the Total Leaf Area (lE_T)

We applied the weighing-lysimeter method developed by Asawa et al. (2012, 2017) for the estimation of lE_T. For this method, a container-grown tree was placed on a platform weighing machine, and the total weight of the tree, container, and soil was measured. All water balances were controlled by an automated irrigation system, and E_T (whole-tree transpiration rate) could be identified from the measured changes in weight and the total leaf area obtained from the laser-scanning data. The weighing machine and container were both enclosed within a structure to protect them from wind, rainfall, and solar radiation. It was confirmed that this method measures the weight change of the target *Z. serrata*, which had a height of 6.4 m, with an accuracy of ± 0.1 kg h^{-1}. This is considered to be of sufficient accuracy to quantify a value of E_T for the analysis of urban tree transpiration, because the weight change by the whole-tree transpiration rate of the target tree was found to be greater than 3 kg h^{-1} during hot, summer days. We applied this weighing-lysimeter method to tree A, which was necessary to estimate lE_T values.

We could not apply the weighing-lysimeter method to tree A′ because of the limitations of cost and experimental effort. Therefore we applied the sap-flow method (Granier's thermal dissipation sensor) (Granier 1987) to tree A′ to check whether the sap flow (transpiration rate) approached zero with the interruption in irrigation during the day, for accurate estimation of g_{hT}. The sap-flow methods are frequently used for studying whole-tree and stand-scale water use (Swanson and Whitfield 1981). However, the sap-flow velocity measured at chest height can be shifted from the actual E_T value by a few hours (e.g., Saugier et al. 1997). In addition, the widely-used Granier's thermal dissipation sensor (Granier 1987) is known to be sensitive to environmental radiation and temperature (Oren et al. 1999; Lu et al. 2004), and this can be problematic in the measurement of isolated (i.e., urban) trees under hot summer conditions. However, tree A′ is a reference tree in our experiment, and the transpiration was minimized by the cessation of irrigation. In the experimental design, we considered that the sap-flow

Fig. 3 Extraction of T_r of the foliage from a thermal image
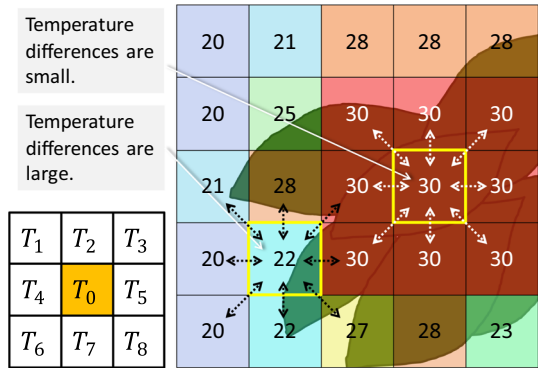
method does not produce a significant error in the estimation of g_{hT} under such drought conditions. On the day of measurement (30 August, 2010), irrigation had been stopped for tree A′ for 7 days, and the pF of the soil was near 4.2, which is the permanent wilting point for plants. The pF is defined as the logarithm of soil matric potential and it was estimated from the measured soil–water content (amplitude-domain reflectometry sensor; Thetaprobe ML2x, Delta-T Devices, Cambridge, UK) and the water retention curve (pF curve) of the sample soil. The result of the soil pF indicated that transpiration was physiologically limited. In addition, the sap flow of tree A′, measured by the Granier's thermal dissipation sensor, was below one-tenth of that of tree A. To verify the assumption that the E'_T value was close to zero, we checked the change in the soil–water content of tree A′ (see Appendix). The measurement for soil–water content strongly indicated that there was no water uptake from the soil to the root, and the transpiration was completely limited. From these points, we comprehensively concluded that the E'_T value of tree A′ was negligible for the g_{hT} estimation.

3.5 Measurement of Foliage Temperature (T_T)

We applied a thermal infrared camera for the measurement of T_T. To ensure the validity of the use of T_r to estimate T_T, as measured by the thermal infrared camera, the following points were considered based on the examination described in Sect. 3.3.

(i) To extract T_r from the foliage in a thermal image, the temperature difference with the background (i.e., the gaps between the leaves and surroundings of the foliage) is needed. Therefore, we set the thermal infrared camera to face the crowns of the trees (the middle height was 5.3 m above ground) from the south and then changed the elevation angle slightly upwards. In more detail, we put the camera with a tripod on the roof of the one-box car used for observation and set the height of the camera at 3.7 m from the ground. The elevation angle was 4°, and the distance between the camera and trees was 10 m. The spatial resolution of the camera is also important in the detection of T_r, noting that the instantaneous field of view of the camera was 2.5 mrad, implying that the spatial resolution of the target from a distance of 10 m was 25 mm. This resolution can distinguish leaves and foliage from the background sky (i.e., pure pixel); however, the boundaries between the foliage and sky are identified as mixed-pixels. Therefore, we extracted the mixed-pixels using a temperature-difference index, D_0, as shown in Fig. 3 and the relation

$$D_0 = \sum_{i=1}^{N} |T_0 - T_i|, \tag{11}$$

where T_0 is the temperature of the centre pixel, T_i is the temperature of the surrounding pixels, and N ($= 8$) is the number of surrounding pixels.

D_0 indicated the sum of the temperature differences of the surrounding eight pixels for the centre pixel. The threshold of D_0 for the extraction was determined for the sample tree, and the mixed-pixels were all deleted from the T_r estimation. The threshold of D_0 was approximately 2.5, and the value was slightly changed with meteorological conditions (e.g., cloud conditions of the background sky) and solar position.

(ii) An emissivity correction for the foliage is needed when T_r is largely different from the behind temperature (T_{Behind}) (i.e., the radiant temperature from the direction of the reflection). In this case, the area behind the infrared camera measurement was populated with tree canopies. The distance between the target trees and tree canopies was 11 m, which is relatively close. This indicates that T_r and T_{Behind} are almost equal, and no emissivity (ε) correction is necessary because the reflected radiation equals the fraction of radiation not emitted ($1-\varepsilon$) by the target (Blonquist Jr. et al. 2009). Therefore, we used the measured T_r value for the T_T value in Eqs. 9 and 10. These two points were considered to ensure an accurate estimation of g_{hT} using the HB-TS method.

(iii) The number of instruments used for measurement should be minimized to reduce instrumental error (systematic error), as discussed in Sect. 3.1. This implies that if different thermal infrared cameras are used for each individual tree, differences in the instrumental feature, condition, or calibration may cause systematic errors in the measured T_r values. Therefore, one thermal infrared camera was used to detect the T_r values of both trees (tree A and tree A′) simultaneously.

(iv) Obtaining an average temperature for all the leaves in the crown is desirable. However, T_r as obtained from the thermal infrared camera is an approximation of the average temperature, because the camera cannot detect all leaf surfaces. We considered that the T_r value gained from the thermal infrared camera could be used as the averaged foliate temperature (T_T) for the following reasons. The sample tree was a young tree and had a relatively low leaf area density ($LAI = 2.4$), implying that there were small leaves hidden from the view of the camera. In addition, the preliminary measurement results for T_r from all four directions using the thermal infrared camera showed that differences in the temperature from the different directions were small (within 0.7 K at maximum). For these reasons, we used the results from one direction (south) for successive measurements.

We also checked whether the T_r values of both trees were identical under dual-irrigated conditions. We obtained the T_r values of both trees on 3 September, under sunny conditions when these trees were fully irrigated. The difference in T_r (tree A′–tree A) was 0.09 ± 0.18 K. This was sufficiently small and supports the assumption that these trees had the same radiometric condition, transpiration, and leaf temperature.

3.6 Meteorological and Measurement Conditions

Meteorological data were obtained in the northern part of the experimental field using a solar radiometer (MS-402, Eko Instruments, Tokyo, Japan), an air temperature sensor (4 wires Pt100Ω, Taiyo Keki, Tokyo, Japan) with an aspirated radiation shield (Model 43502, R. M. Young Co., Traverse, Michigan, USA), a relative humidity sensor (CS215, Campbell Scientific, Logan, Utah, USA), a tipping bucket gauge for precipitation (TE525MM, Campbell Scientific), a three-dimensional ultrasonic anemometer (Model 81000, R. M. Young Co.), and a photosynthetically active radiation (PAR) sensor (LI-190, Li-Cor Inc., Lincoln, Nebraska, USA). This position was set as the reference position. To analyze the effects of airflow on

T_r and g_{hT}, the anemometer was located 4.3 m from the *Z. serrata* (Fig. 1). This location was determined to be as close as possible to the tree while minimizing the drag-force effect that the tree would have on the wind measurements. The height of the anemometer was 4 m, similar to the height of the centre of the tree crown.

Measurements were carried out in the summer of 2010, which was hot and dry across Japan, and the longest stretch of sun at the study site was 18 days, from 21 August through 7 September. We irrigated approximately 30–50 kg m^{-2} of soil daily, determined by using the E_T values from the preceding days, which was sufficient to compensate for the water loss from daily transpiration. We confirmed that ample irrigation was not problematic for the E_T estimation, because any excess of water over the field capacity was soon discharged. We irrigated at night-time (from 0300 LST to 0500 LST) almost every day during the season, except the period of the dry-down experiments on tree A. Times are expressed in local standard time (LST = UTC + 9 h). For the dry-down experiments, irrigation was stopped for two to four successive days to ascertain the effects of drought stress while minimizing the damage to the growth of the tree. For tree A′, irrigation was stopped for several successive days to minimize E_T' and lE_T' for the HB-TS method, as explained in Sects. 3.3 and 3.4. The condition of these trees was carefully checked during the test period to avoid damaging the tree (e.g., via withering or defoliation).

We paid close attention to selecting a date for the estimation of g_{hT} and heat fluxes as we needed to use comparable dates for the two different conditions. To estimate g_{hT} using the HB-TS method, we selected the date of 30 August for tree A and tree A′. 30 August experienced a clear sky during the day and the E_T' value of tree A′ was confirmed to be minimized, as checked by the sap flow and soil–water content by the method explained in Sect. 3.4. In contrast, tree A showed almost maximum transpiration owing to the ample irrigation over the four successive days. This means we waited for both conditions, minimizing the transpiration of tree A′ and recovering that of tree A after the dry-down experiment by carefully checking the weather and tree conditions. Consequently, we could make a large difference in E_T and T_T between these trees as expected.

4 Results

4.1 Foliage Temperature (T_T)

Figure 4 shows an example of the thermal images for tree A and tree A′, and Fig. 5 shows the results of averaged foliage temperatures (T_T, T_T') for tree A and tree A′ on 30 August obtained from the thermal image (e.g., Fig. 4). It is confirmed that the T_T value was a maximum of 1 K higher than T_a, and the T_T' value was 3 K higher than T_a. This means that the transpiration from tree A caused a decrease in the foliage temperature of up to 2 K. The results for (T_T–T_a) and (T_T'–T_a) show that these trends corresponded significantly with the solar radiation. Increases in solar radiation caused simultaneous increases in the foliage temperature. In particular, the effect of an instantaneous reduction in solar radiation between 0900 LST and 1000 LST was reflected as a reduction in the foliage temperatures. The result of (T_T'–T_T) shows that there was little difference between T_T' and T_T during the night-time. This means that the radiation transfer characteristics and the g_{hT} value were equivalent for the two sample trees, and only E_T caused a difference in the foliage temperatures. During the daytime, the changing trend of (T_T'–T_T) corresponded well with the E_T value. These results support the

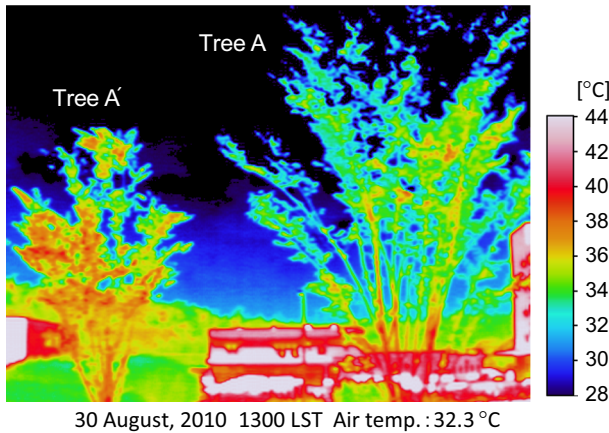30 August, 2010 1300 LST Air temp. : 32.3 °C

Fig. 4 Thermal images for the two trees under different irrigation conditions

theoretical and literature-derived idea in Sect. 3.3 that g_{hT} can be estimated from Eq. 9 with $(T_T{}'-T_T)$ and E_T. Thus, H_T can also be estimated using these results with Eq. 10.

4.2 Boundary-Layer Heat Conductance of the Total Leaf Area (g_{hT})

Figure 6 shows the results for the g_{hT} value estimated in Asawa et al. (2016) and the relationship with the wind speed outside the tree crown. The wind speed was estimated via the composition of the three-dimensional vectors of the instantaneous velocity components, averaged over 1 h. If the lE_T value of tree A and the foliage temperature difference between two trees $(T_T{}'-T_T)$ is small, the estimation error for g_{hT} should become large. Therefore, we used the data when $lE_T > 50$ W m^{-2} and the temperature difference $(T_T{}'-T_T) > 1$ K, respectively, for the g_{hT} estimation. In the figure, the g_h value of an individual leaf from tree A was also plotted for the comparison. The wind speed for the individual leaf was measured at a distance 0.3 m from the leaf. The wind speed ranged from 1.1 to 2.5 m s^{-1} for the tree crown, and from 0.4 to 2.0 m s^{-1} for the individual leaf, respectively. The main findings with this figure obtained from Asawa et al. (2016) are as follows.

The g_{hT} value of the tree crown and the g_h value of the individual leaf both increased with the wind speed, and the plots almost overlapped. By applying linear regression, the slopes were found to be almost equivalent, and the intercepts differed by only 1 W m^{-2} K^{-1}. This difference is considered to be derived from the difference in the measurement positions of wind speed (i.e., the wind speed outside the tree crown was higher than that near the leaf owing to the drag-force effect of the tree crown). The coefficients of determination, R^2 were 0.56 for the tree crown and 0.77 for the individual leaf. Although the R^2 value of the tree crown is smaller than that of the individual leaf, there is a clear relationship between the wind speed and g_{hT} for the tree crown. These results show that the g_{hT} value was effectively estimated with the HB-TS method by using the E_T value and the foliage temperature difference $(T_T{}'-T_T)$.
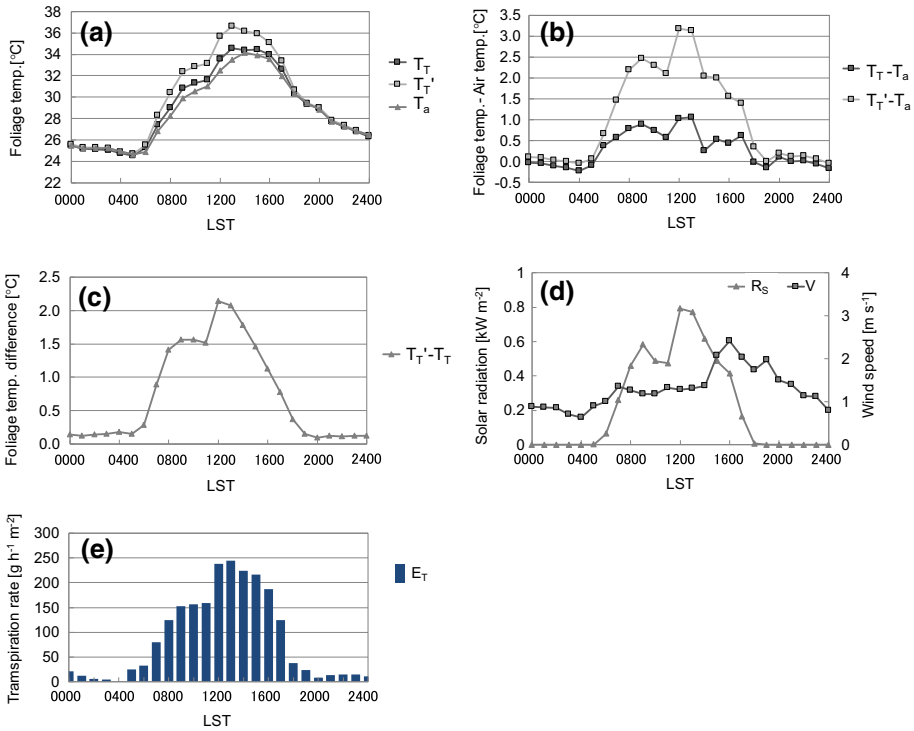
Fig. 5 Averaged foliage temperatures for tree A and tree A′ on 30 August obtained from infrared thermography: **a** averaged foliage temperatures (T_T, $T_T{'}$); **b** difference between averaged foliage temperatures and air temperature ($T_T{-}T_a$, $T_T{'}{-}T_a$); **c** difference in averaged foliage temperature between tree A′ and tree A ($T_T{'}{-}T_T$); **d** solar radiation per ground area (R_S) and wind speed (V); and **e** whole-tree transpiration rate of tree A (E_T) per hour per leaf area are shown
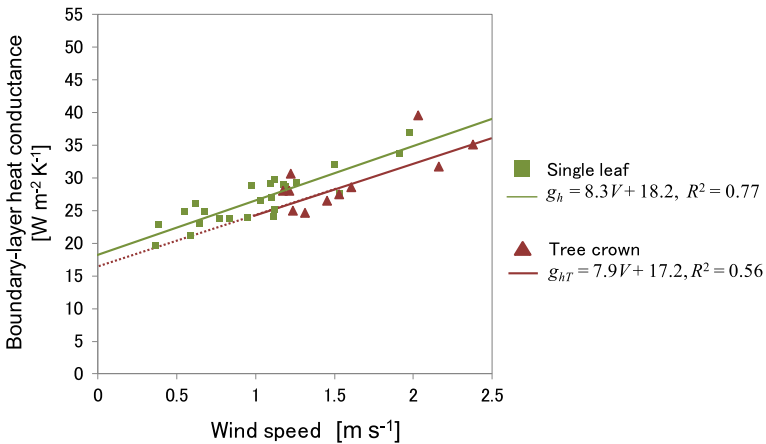

Fig. 6 Estimation result of the boundary-layer heat conductance (g_{hT}) per leaf area of the tree crown with the relationship to the wind speed outside the tree crown. The g_h value of an individual leaf of tree A was also plotted. Both results were estimated in Asawa et al. (2016)
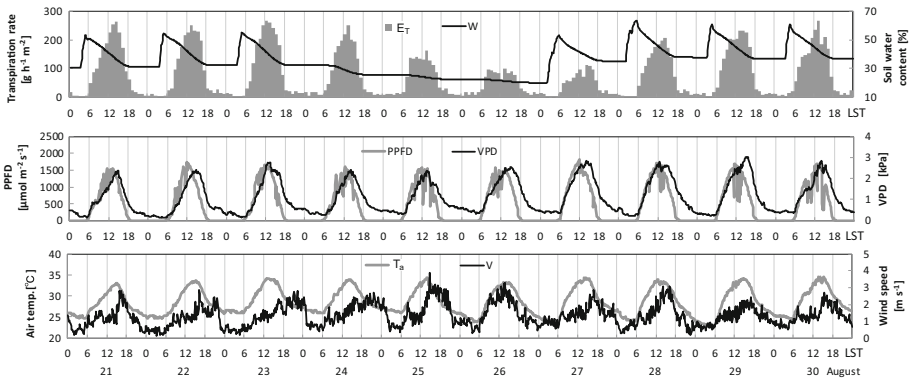
Fig. 7 Whole-tree transpiration rate (E_T) of tree A per hour per leaf area from 21 August to 30 August. Soil–water content (W), photosynthetic photon flux density ($PPFD$), vapour-pressure deficit (VPD), air temperature (T_a), and wind speed (V) are also shown

4.3 Whole-Tree Transpiration Rate (E_T)

Figure 7 shows the E_T value of tree A from 21 to 30 August, 2010. Here, E_T was estimated per hour per leaf area to check hourly and daily changes. In this figure, soil–water content, photosynthetic photon flux density, vapour-pressure deficit, air temperature, and wind speed are also shown. Clear skies and high temperatures (>32 °C) occurred over the entire period. For the dry-down experiment within the period, irrigation was stopped from 24 to 26 August, and was continued on the other days. From 21 to 23 August, when sufficient irrigation had been supplied, the E_T value increased with the photosynthetic photon flux density and vapour-pressure deficit. A peak in E_T occurred at around midday, from 1300 LST to 1500 LST. The timing was close to that of the vapour-pressure deficit and was delayed compared with the photosynthetic photon flux density. The E_T value reached a peak of over 250 g h^{-1} m^{-2} during the day. The same tendencies were obtained on 29 and 30 August, when sufficient irrigation was also supplied after the dry-down experiment. At night-time, the E_T value was close to 5 g h^{-1} m^{-2} for the entire period. During the dry-down experiment, the E_T value decreased with the reduction in the soil–water content. The reduction of soil–water content corresponded with the reduction in E_T. This result clearly shows that tree A closed stomata because of the drought stress during the dry-down experiment. The E_T value on 26 August was approximately one-third that on 23 August, with the pF value of the soil of tree A estimated at 4.5 on 26 August. We judged that the soil–water condition reached the permanent wilting point of plants on that day (26 August), and so resumed irrigation the next day (27 August). After 27 August, the E_T value recovered gradually within 3 days with sufficient soil water. By 29 August, the E_T value was well recovered. These results show that the change in E_T was adequately measured along with the soil–water content by the weighing lysimeter, and the E_T value differed three times under different soil–water content during successive sunny days.

4.4 Sensible and Latent Heat Fluxes of the Total Leaf Area (H_T, lE_T)

From the results of the T_T, g_{hT}, and E_T values of tree A, we estimated H_T and lE_T over the total leaf area to the atmosphere. We applied these results to Eq. 10 to estimate H_T. We compared two different days: 30 August, on which E_T was large with sufficient irrigation

and higher soil–water content, and 26 August, on which E_T was small without irrigation and soil–water content was at its lowest because of the dry-down experiment. Figure 8e, f shows the H_T and lE_T values of tree A for both days. In this figure, global solar radiation per leaf area and wind speed near the tree (Fig. 8a, b), the difference between averaged foliage temperatures and air temperature ($T_T–T_a$), and the boundary-layer heat conductance (g_{hT}) over the total leaf area (Fig. 8c, d), are also depicted. On 26 August, the wind speed was higher than on 30 August; thus, the g_{hT} value was also larger. The value of ($T_T–T_a$) was greater on 26 August than on 30 August during the daytime owing to drought stress caused by the cease in irrigation. On 30 August, the peak of lE_T was over 80 W m^{-2} at 1300 LST, and this value was approximately 2.5 times larger than that of H_T. The appearance of two peaks for H_T was equivalent to that of the solar radiation. The second peak of H_T appeared at 1300 LST, and the tendencies of H_T and lE_T were similar. These results imply that the solar energy received by the total leaf area was mainly converted to lE_T, and the rest was converted to H_T. During the daytime (from 0900 LST to 1600 LST), the Bowen ratio ($\beta = H_T/lE_T$) was 0.29 on average. During the night-time, the H_T and lE_T values were both very small, and H_T was negative. In contrast, for 26 August, the peak of H_T was approximately 80 W m^{-2}, 2.5 times larger than that of lE_T. The appearance of two peaks and the tendency of H_T were similar to those of the solar radiation. The β value was 2.2 during the daytime. The tendencies of H_T and lE_T reversed between the 2 days under different irrigation conditions, and the β value largely changed along with irrigation and soil–water conditions.

5 Discussion

5.1 Energy Closure

For energy flux observations over forest sites, energy closure is verified by comparing the surface energy flux of $H_T + lE_T$ with the available energy ($R_n - G$, where R_n is the net radiation and G is the storage heat flux) (Wilson et al. 2002b). The error shown in the $H_T + lE_T$ estimation is known as the "imbalance problem" or "energy closure problem" (e.g., Mahrt 1998; Moriwaki and Kanda 2004). Wilson et al. (2002b) reported that the lack of energy closure at FLUXNET sites was about 20% on average. In contrast to energy flux observations over forest sites, the present observation cannot apply the same energy closure method because one-dimensional energy fluxes cannot be assumed over the total leaf area of an isolated tree. Therefore, we directly compared $H_T + lE_T$ between different days with similar solar radiation and different water content conditions (30 August and 26 August).

Table 1 shows the daily solar radiation (R_S), daily H_T, daily lE_T, and daily $H_T + lE_T$ for both days. For the total leaf area of an isolated tree, $R_n–G$ is not quantifiable. Therefore, R_S was used to check the similarity of the radiation environment (R_n) between the 2 days. G is considered to be very small and negligible for the foliage of the tree crown, because changes in T_T closely followed corresponding changes in R_S, without any significant delays, as shown in Fig. 5. From Table 1, although the daily H_T and daily lE_T values changed significantly because of different soil–water content (W) on the 2 days, the difference in daily $H_T + lE_T$ was approximately 1%. The 2 days had similar daily R_S values. There is a limitation in that this is only the comparison between 2 days that had full sets of measurements; however, the energy closure is more precise than that of flux observations over forest sites (Wilson et al. 2002b). This result shows the energy was appropriately close on the 2 days, and this result is sufficiently accurate for discussing the characteristics of H_T and lE_T.
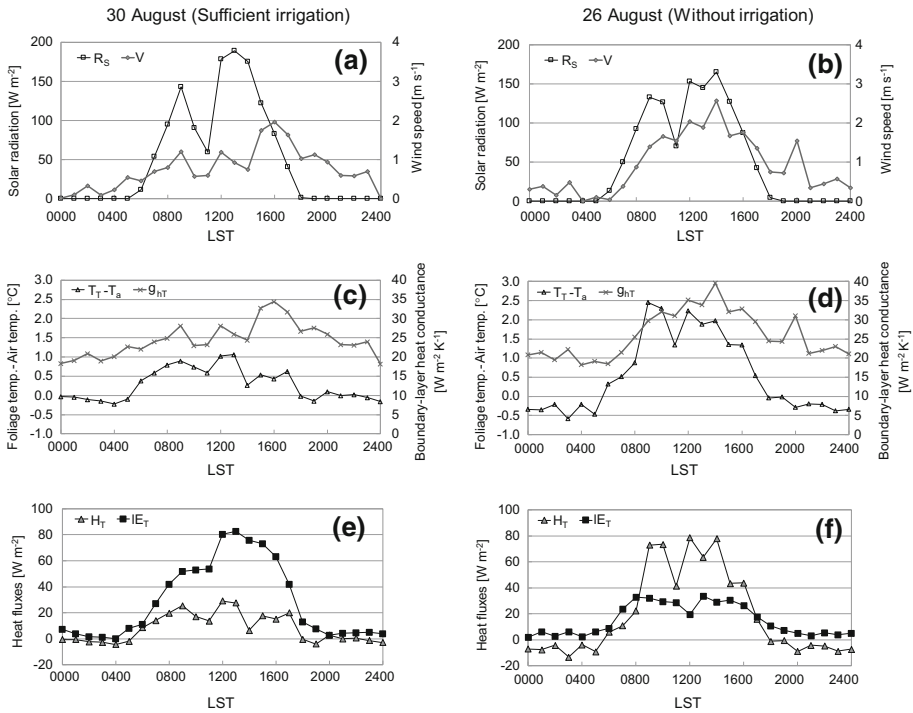
Fig. 8 Estimation results of the sensible heat flux (H_T) and latent heat flux (lE_T) per leaf area under different irrigation conditions (30 August with sufficient irrigation and 26 August without irrigation): **a**, **b** show solar radiation per leaf area (R_S) and wind speed (V); **c**, **d** show the difference between averaged foliage temperatures and air temperature ($T_T - T_a$), and boundary-layer heat conductance (g_{hT}) over the total leaf area; and **e**, **f** show sensible heat flux (H_T) and latent heat flux (lE_T)

Table 1 Daily solar radiation (R_S), daily H_T, daily lE_T, and daily $H_T + lE_T$ on 30 August and 26 August. All results were estimated per leaf area

Daily amount (MJ m^{-2} day^{-1})	30 August (sufficient irrigation, larger W)	26 August (without irrigation, smaller W)	Difference (30 August–26 August)
Daily R_S	4.47	4.36	0.11
Daily H_T	0.77	1.97	− 1.2
Daily lE_T	2.40	1.16	1.24
Daily $H_T + lE_T$	3.17	3.13	0.04

5.2 Comparison with Flux Data over Forests

Wilson et al. (2002a) reported the results of energy partitioning between lE and H during the warm season at FLUXNET (a global network of micrometeorological flux measurement based on the eddy-covariance method) sites with different climatic regions and forest types. Of the different forest and agricultural sites, deciduous forest had the lowest value of β (0.25–0.50), equivalent to that of agricultural sites. The value of β obtained in the present study is 0.29 under irrigated conditions, which is almost the same as that of the deciduous

forest sites. For the interannual variation in β at individual sites, drought was one expected source (Wilson et al. 2002a). Baldocchi (1997) observed the effects of soil moisture deficits and high temperature stress on lE values over a temperate broad-leaved forest. There was no great change in lE values from the growing season (well-watered season) to the drought season, despite large changes in the canopy drought-stress index. Even during a period in which the lowest pre-down water potentials were experienced, the lE values were 25% lower than that during the well-watered period, as the forest had experienced a prolonged period of soil-moisture deficit. The same finding was also reported by Greco and Baldocchi (1996) and Oliphant et al. (2004), and the effectiveness of deep roots in sourcing water stored in the soil column was also suggested (Baldocchi 1997; Oliphant et al. 2004). Wilson and Baldocchi (2000) reported that the daytime β value during the drought stress period (in 1995) for broad-leaved temperate deciduous forest was about twice that during the wetter periods (in 1996 and 1997). In contrast, the present study shows that the lE_T value was reduced by 60% owing to drought stress for an isolated tree. In addition, the daytime β value on the drought day (26 August) was 7.6 times larger than that on the wetter day (30 August). The great reduction in lE_T can be explained by the characteristics of the urban-unique conditions of tree planting (i.e., drought stress from a large vapour-pressure deficit and limits to water supply, soil volume, and root space) (see Sect. 5.3). For a deciduous forest, such a dramatic change in H_T and lE_T was only observed before and after leaf emergence within about a 6–8 week period (Wilson and Baldocchi 2000). However, the present results suggest that dramatic changes to H_T and lE_T for isolated trees can occur within several days in urban environments.

5.3 Comparison with Flux Data for Urban Sites

Next, our results are compared with flux measurements for urban sites. The value for β in previous studies mainly ranged between 1 and 5 for daytime conditions at different urban sites (Grimmond et al. 2009); meanwhile, in the present study, the β value was 2.2 under drought conditions, which is within the range obtained previously at urban sites. Moriwaki and Kanda (2004) reported that β at a residential area of Tokyo, Japan was 1.8 during daytime summer, which was smaller than the β value for the drought condition in the present study. This means that the trees do not cool the urban atmosphere because of low transpiration rates under drought conditions; thus, urban trees reach drought conditions within a short period. Urban trees can be exposed to drought stress because of both high air temperatures and reduced water availability (Gillner et al. 2013; Savi et al. 2015), because impervious pavements prevent the infiltration of rainwater resulting in significantly lower soil–water content beneath these pavements (Morgenroth et al. 2013). In addition, compacted urban soils reduce infiltration by water and increase surface runoff (Yang and Zhang 2011). These phenomena are collectively known as the anthropogenic sealing of soils (Scalenghe and Marsan 2009). The present results, together with these findings, indicate the importance of regular irrigation or the sufficient utilization of rainwater to obtain a cooling effect from urban trees as well as maintain the health of the trees.

5.4 Oasis Effect

Moriwaki and Kanda (2004) reported that the lE value over a suburban area in Tokyo, Japan, was 183 W m^{-2} at noon in summer, and was considered to be the area-averaged flux, including fluxes from both natural and artificial surfaces. The authors suggested that the lE value per unit

of natural coverage (e.g., trees, shrubs, and bare soil) should be at 631 W m^{-2}, considering that 29% of the total land area was natural coverage, and the relatively high amount of evaporation is consistent with the oasis effect. For the present result, the lE_T value per unit ground area on the horizontal plane was a maximum of 400 W m^{-2} under irrigated conditions and 160 W m^{-2} under drought conditions. These results do not include evaporation from the ground; however, these results have much lower values than those observed by Moriwaki and Kanda ([2004](#)) at an urban site. The present results are inconsistent with this result. The verification of consistency between the transpiration of trees and area-averaged lE over urban sites is a possible subject for future research. We consider this inconsistency to be a very important topic for urban flux studies. Here, the next research question has been derived: what is the main source of transpiration in urban sites, indicated by Moriwaki and Kanda ([2004](#))?

6 Conclusions

We have quantified both the sensible heat flux (H_T) and latent heat flux (lE_T) of the total leaf area of *Z. Serrata* in an outdoor environment during the Japanese summer. We applied the weighing-lysimeter method to quantify the whole-tree transpiration rate (E_T) and latent heat flux lE_T over successive days with different soil–water conditions. To estimate the boundary-layer heat conductance (g_{hT}) and H_T, we carefully applied the scaling-up approach of the heat-balance two-state (HB-TS) method from single leaves to a tree crown based on comprehensive literature reviews and theoretical considerations. Two sample trees were selected for the estimation, with similar crown shapes and leaf areas; the difference in leaf area was 10% between the two trees, expected to result in a 10% error in H_T estimation. We varied soil–water conditions for the trees by controlling irrigation conditions to achieve the different foliage temperatures (T_T) and whole-tree transpiration (E_T) required for the HB-TS method.

The measurement of E_T during the dry-down experiment showed that its change corresponded well with the soil–water content, and E_T was successfully quantified using the weighing-lysimeter method. The E_T values differed three times during the dry-drown experiment within several days. We compared H_T and lE_T between two different days with different irrigation and soil–water conditions during the dry-down experiment. The most important result was that the tendencies of H_T and lE_T were reversed between these 2 days, and the Bowen ratio ($\beta = H_T / lE_T$) dramatically changed. The β value was 0.29 for daytime with adequate irrigation, for the largest E_T value, and almost the same as that for deciduous forest sites (Wilson et al. [2002a](#)). In contrast, the β value was 2.2 during the daytime under drought conditions, with the smallest E_T value, and similar to results obtained from urban sites (Grimmond et al. [2009](#)). From these informative findings, we indicated that the β values of isolated trees in urban sites can change between forest-like values and urban-like values within a short time period owing to urban-unique conditions (e.g., large vapour-pressure deficit, limited water supply and root space, impervious pavements, and strong soil compaction). We suggested the importance of regular irrigation or the effective utilization of rain water not only for healthy growth of urban trees but also for allowing the cooling effect of the trees from transpiration. These data are expected to be applied for the optimization of irrigation control in urban landscapes, maintaining a cooling effect while minimizing the use of water resources. For urban meteorology, these data are expected to be used for the
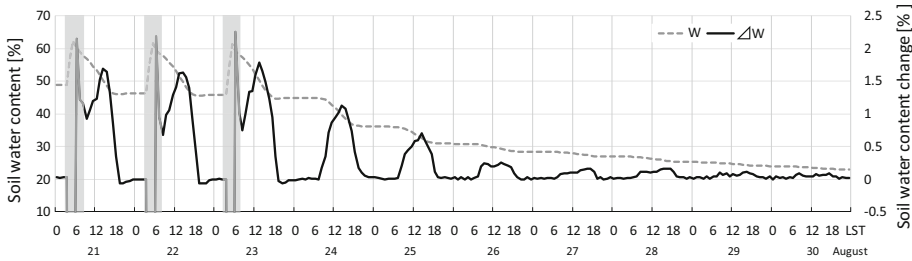
Fig. 9 Measurement results of soil water content (W) and soil water content change per hour (ΔW) for tree A′. Gray bands show the period of irrigation

parameterization of g_{hT}, the modelling of the soil–plant–atmosphere continuum for urban trees, and the validation of simulated H_T and lE_T under different irrigation conditions.

Appendix

As shown in Fig. 7, the soil–water content corresponded well with the transpiration rate, as there was no intake nor drainage of water without transpiration when the irrigation was stopped. Figure 9 shows the measurement results of soil–water content and soil–water content change per hour for tree A′. For the irrigated period until 23 August, the soil–water content change was over 1.5% per hour during the daytime owing to the transpiration. The value decreased after the cease in irrigation on 24 August. On 27 August, the value became one-tenth of that on the irrigated days. To make sure the transpiration was completely (biophysiologically) limited and negligible for g_{hT} and H_T estimation, we waited three more days. On 30 August, the value became one-twentieth of that on the irrigated days, as we expected. Therefore, we judged this day to be applicable to the estimation.

References

Anderson DE, Verma SB, Rosenberg NJ (1984) Eddy correlation measurements of CO_2, latent heat, and sensible heat fluxes over a crop surface. Boundary-Layer Meteorol 29:263–272

Asawa T, Hoyano A, Nakaohkubo K (2008) Thermal design tool for outdoor spaces based on heat balance simulation using a 3D-CAD system. Build Environ 43:2112–2123

Asawa T, Hoyano A, Shimizu K, Kubota M (2012) Measuring method for transpiration of a single tree using weighing machine and confirmation of its accuracy. J Jpn Soc Reveg Technol 38:67–72 **(in Japanese with English summary)**

Asawa T, Hoyano A, Shimizu K, Kubota M (2014a) Analysis of transpiration characteristics of Zelkova serrata in summer using a weighing machine. J Jpn Soc Reveg Technol 39:534–541 **(in Japanese with English summary)**

Asawa T, Hoyano A, Oshio H, Honda Y, Shimizu K, Kubota M (2014b) Terrestrial LiDAR-based estimation of the leaf area density distribution of an individual tree and verification of its accuracy. In: Proceedings of international symposium on remote sensing (electronic proceedings)

Asawa T, Fujiwara K, Hoyano A, Shimizu K (2016) Convective heat transfer coefficient of crown of *Zelkova serrata*. J Environ Eng (Trans AIJ) 720:235–245 **(in Japanese with English summary)**

Asawa T, Kiyono T, Hoyano A (2017) Continuous measurement of whole-tree water balance for studying urban tree transpiration. Hydrol Process 31:3056–3068

Balding FR, Cunningham GL (1976) A comparison of heat transfer characteristics of simple and pinnate leaf models. Bot Gaz 137:65–74

Baldocchi DD (1997) Measuring and modelling carbon dioxide and water vapour exchange over a temperate broad-leaved forest during the 1995 summer drought. Plant, Cell Environ 20:1108–1122

Baldocchi DD, Luxmoore RJ, Hatfield JL (1991) Discerning the forest from the trees: an essay on scaling canopy stomatal conductance. Agric For Meteorol 54:197–226

Baldocchi DD, Law BE, Anthoni PM (2000) On measuring and modeling energy fluxes above the floor of a homogeneous and heterogeneous conifer forest. Agric For Meteorol 102:187–206

Bastiaanssen WGM (2000) SEBAL-based sensible and latent heat fluxes in the irrigated Gediz basin, Turkey. J Hydrol 229:87–100

Blad BL, Rosenberg NJ (1976) Evaluation of resistance and mass transport evapotranspiration models requiring canopy temperature data. Agron J 68:764–769

Blonquist JM Jr, Norman JM, Bugbee B (2009) Automated measurement of canopy stomatal conductance based on infrared temperature. Agric For Meteorol 149:1931–1945

Brenner AJ, Jarvis PG (1995) A heated leaf replica technique for determination of leaf boundary layer conductance in the field. Agric For Meteorol 72:261–275

Bruse M, Fleer H (1998) Simulating surface-plant-air interactions inside urban environments with a three dimensional numerical model. Environ Model Softw 13:373–384

Cammalleri C, Anderson MC, Ciraolo G, D'Urso G, Kustas WP, Minacapilli GL (2012) Applications of a remote sensing-based two-source energy balance algorithm for mapping surface fluxes without in situ air temperature observations. Remote Sens Environ 124:502–515

Campbell CS, Norman JM (1998) An introduction to environmental biophysics. Springer, New York

Chen C (2003) Development of a heat transfer model for plant tissue culture vessels. Biosyst Eng 85:67–77

Chen F, Kusaka H, Bornstein R, Ching J, Grimmond CSB, Grossman-Clarke S, Loridan T, Manning K, Martilli A, Miao S, Sailor D, Salamanca F, Taha H, Tewari M, Wang X, Wyszogrodzky A, Zhang C (2011) The integrated WRF/urban modelling system: development, evaluation, and applications to urban environmental problems. Int J Climatol 31:273–288

Choudhury BJ, Reginato RJ, Idso SB (1986) An analysis of infrared temperature observations over wheat and calculation of latent heat flux. Agric For Meteorol 37:75–88

Clear RD, Gartland L, Winkelmann FC (2003) An empirical correlation for the outside convective air-film coefficient for horizontal roofs. Energy Build 35:797–811

Colaizzi PD, Kustas WP, Anderson MC, Agam N, Tolk JA, Evett SR, Howell TA, Gowda PH, O'Shaughnessy SA (2012) Two-source energy balance model estimates of evapotranspiration using component and composite surface temperatures. Adv Water Resour 50:134–151

Cregg B (1995) Plant moisture stress of green ash trees in contrasting urban sites. J Arboric 21:271–276

Defraeye T, Verboven P, Ho QT, Nicolai B (2013) Convective heat and mass exchange predictions at leaf surfaces: applications, methods and perspectives. Comput Electron Agric 96:180–201

DeRocher TR, Walker RF, Tausch RJ (1995) Estimating whole-tree transpiration of *Pinus monophylla* using a steady-state porometer. J Sustain For 3(1):85–99

Edwards W (1986) Precision weighing lysimetry for trees, using a simplified tared-balance design. Tree Physiol 1:127–144

Gillner S, Vogt J, Roloff A (2013) Climatic response and impacts of drought on oaks at urban and forest sites. Urban For Urban Green 12:597–605

Granier A (1987) Evaluation of transpiration in a Douglas-fir stand by means of sap flow measurements. Tree Physiol 3:309–320

Greco S, Baldocchi DD (1996) Seasonal variations of CO_2 and water vapour exchange rates over a temperate deciduous forest. Glob Change Biol 2:183–197

Grimmond CSB, Lietzke B, Vogt R, Young D, Marras S, Spano D (2009) Inventory of current state of empirical and modeling knowledge of energy, water and carbon sinks, sources and fluxes. BRIDGE-Collaborative Project. Contract no.: 211345. http://bridge-fp7.eu/images/reports/BRIDGE%20D.2.1.pdf

Hagishima A, Tanimoto J (2003) Field measurement for estimating the convective heat transfer coefficient at building surfaces. Build Environ 38:873–881

Hagishima A, Narita K, Tanimoto J (2007) Field experiment on transpiration from isolated urban plants. Hydrol Process 27:1217–1222

Hasebe T (1984) Convection coefficient of transfer across the boundary layer on plant leaf surface. J Agric Meteorol 40:63–72

Hatfield JL (1983) The utilization of thermal infrared radiation measurements from grain sorghum crops as a method of assessing their irrigation requirements. Irrig Sci 3:259–268

Hosoi F, Omasa K (2006) Voxel-based 3-D modeling of individual trees for estimating leaf area density using high-resolution portable scanning Lidar. IEEE Trans Geosci Remote Sens 44:3610–3618

Ito N, Kimura K, Oka J (1972) A field experiment study on the convective heat transfer coefficient on exterior surface of a building. ASHRAE Trans 78:184–191

Jackson RD, Idso SB, Reginato RJ, Pinter PJ Jr (1981) Canopy temperature as a crop water stress indicator. Water Resour Res 17:1133–1138

Jones HG (2004) Application of thermal imaging and infrared sensing in plant physiology and ecophysiology. Adv Bot Res 41:107–163

Jones HG, Hutchinson PA, May T, Jamali H, Deery DM (2018) A practical method using a network of fixed infrared sensors for estimating crop canopy conductance and evaporation rate. Biosyst Eng 165:59–69

Kagotani Y, Nishida K, Kiyomizu T, Sasaki K, Kume A, Hanba Y (2015) Photosynthetic responses to soil water stress in summer in two Japanese urban landscape tree species (*Ginkgo biloba* and *Prunus yedoensis*): effects of pruning mulch and irrigation management. Trees 30:697–708

Kalma JD, McVicar TR, McCabe MF (2008) Estimating land surface evaporation: a review of methods using remotely sensed surface temperature data. Surv Geophys 29:421–469

Kanda M (2007) Progress in urban meteorology: a review. J Meteorol Soc Jpn 85B:363–383

Kitano M, Tateishi J, Eguchi H (1995) Evaluation of leaf boundary layer conductance of a whole plant by application of abscisic acid inhibiting transpiration. Biotronics 24:51–58

Kjelgren R, Clark J (1993) Growth and water relations of *Liquidambar styraciflua* L. in an urban park and plaza. Trees 7:195–201

Kumar A, Barthakur N (1971) Convective heat transfer measurements of plants in a wind tunnel. Boundary-Layer Meteorol 2(2):218–227

Kustas WP, Norman JM (2000) A two-source energy balance approach using directional radiometric temperature observations for sparse canopy covered surfaces. Agron J 92:847–854

Kustas WP, Choudhury BJ, Moran MS, Reginato RJ, Jackson RD, Gay LW, Weaver HL (1989) Determination of sensible heat flux over sparse canopy using thermal infrared data. Agric For Meteorol 44:197–216

Kustas WP et al (2012) Evaluating the two-source energy balance model using local thermal and surface flux observations in a strongly advective irrigated agricultural area. Adv Water Resour 50:120–133

Landsberg JJ, Powell DBB (1973) Surface exchange characteristics of leaves subject to mutual interference. Agric Meteorol 12:169–184

Law BE, Cascatti A, Baldocchi DD (2001) Leaf area distribution and radiative transfer in open-canopy forests: implications for mass and energy exchange. Tree Physiol 21:777–787

Leverenz J, Deans J, Ford E, Jarvis P, Milne R, Whitehead D (1982) Systematic spatial variation of stomatal conductance in a Sitka Spruce Plantation. J Appl Ecol 19:835–851

Lhomme JP, Katerji N, Bertolini JM (1992) Estimating sensible heat flux from radiometric temperature over crop canopy. Boundary-Layer Meteorol 61:287–300

Lhomme JP, Monteny B, Amadou M (1994) Estimating sensible heat flux from radiometric temperature over sparse millet. Agric For Meteorol 68:77–91

Lorite I, Santos C, Teti L, Fereres E (2012) Design and construction of a large weighing lysimeter in an almond orchard. Span J Agric Res 10:238–250

Loveday DL, Taki AH (1996) Convective heat transfer coefficients at a plane surface on a full-scale building façade. Int J Heat Mass Transf 39:1729–1742

Lu P, Urban L, Zhao P (2004) Granier's thermal dissipation probe (TDP) method for measuring sap flow in trees: theory and practice. Acta Bot Sin 46:631–646

Mahrt L (1998) Flux sampling errors for aircraft and towers. J Atmos Oceanic Technol 15:416–429

Martin TA et al (1999) Boundary layer conductance, leaf temperature and transpiration of *Abies amabilis* branches. Tree Physiol 19(7):435–443

McCarthy H, Pataki D (2010) Drivers of variability in water use of native and non-native urban trees in the greater Los Angeles area. Urban Ecosyst 13:393–414

Mecikalski JR, Diak GR, Anderson MC, Norman JM (1999) Estimating fluxes on continental scales using remotely sensed data in an atmospheric-land exchange model. J Appl Meteorol 38:1352–1369

Miglietta F, Gioli B, Brunet Y, Hutjes RWA, Matese A, Sarrat C, Zaldei A (2009) Sensible and latent heat flux from radiometric surface temperatures at the regional scale: methodology and evaluation. Biogeosciences 6:1975–1986

Ministry of Land, Infrastructure, Transport and Tourism (2005) Estimation standard of civil works. MLIT, Tokyo **(in Japanese)**

Morgenroth J, Buchan G, Scharenbroch BC (2013) Belowground effects of porous pavements—soil moisture and chemical properties. Ecol Eng 51:221–228

Moriwaki R, Kanda M (2004) Seasonal and diurnal fluxes of radiation, heat, water vapor, and carbon dioxide over a suburban area. J Appl Meteorol 43:1700–1710

Murphy CE, Knoerr KR (1977) Simultaneous determination of the sensible and latent heat transfer coefficients for tree leaves. Boundary-Layer Meteorol 11:223–241

National Institute for Land and Infrastructure Management (2014) Street tree of Japan VI. NILIM Report 506 **(in Japanese)**

Norman JM, Kustas WP, Humes KS (1995) Source approach for estimating soil and vegetation energy fluxes in observations of directional radiometric surface temperature. Agric For Meteorol 77:263–293

Oke TR (1987) Boundary layer climates, 2nd edn. Routledge, London

Oliphant AJ et al (2004) Heat storage and energy balance fluxes for a temperate deciduous forest. Agric For Meteorol 126:185–201

Oren R, Phillips N, Ewers B, Pataki D, Megonigal J (1999) Sap-flux-scaled transpiration responses to light, vapor pressure deficit, and leaf area reduction in a flooded *Taxodium distichum* forest. Tree Physiol 19:337–347

Oshio H, Asawa T, Hoyano A, Miyasaka S (2015) Estimation of the leaf area density distribution of individual trees using high-resolution and multi-return airborne LiDAR data. Remote Sens Environ 166:116–125

Osone Y, Kawarasaki S, Ishida A, Kikuchi S, Shimizu A, Yazaki K, Matsumoto G (2014) Responses of gas-exchange rates and water relations to annual fluctuations of weather in three species of urban street trees. Tree Physiol 34:1056–1068

Parker GG, Harmon ME, Lefsky MA, Chen J, Pelt RV, Weiss SB, Thomas SC, Winner WE, Shaw DC, Franklin JF (2004) Three-dimensional structure of an old-growth Pseudotsuga-tsuga canopy and its implications for radiation balance, microclimate, and gas exchange. Ecosystems 7:440–453

Parkhurst DF et al (1968) Wind-tunnel modelling of convection of heat between air and broad leaves of plants. Agric Meteorol 5(1):33–47

Parlange J-Y, Waggoner PE (1972) Boundary layer resistance and temperature distribution on still and flapping leaves II. Field experiments. Plant Physiol 50(1):60–63

Paul G, Gowda PH, Prasad PVV, Howell TA, Staggenborg SA, Neale CMU (2013) Lysimetric evaluation of SEBAL using high resolution airborne imagery from BEAREX08. Adv Water Resour 59:157–168

Roberts J (1983) Forest transpiration: a conservative hydrological process? J Hydrol 66:133–141

Saugier B, Granier A, Pontailler J, Dufrene E, Baldocchi DD (1997) Transpiration of a boreal pine forest measured by branch bag, sap flow and micrometeorological methods. Tree Physiol 17:511–519

Savi T, Bertuzzi S, Branca S, Tretiach M, Nardini A (2015) Drought-induced xylem cavitation and hydraulic deterioration: risk factors for urban trees under climate change? New Phytol 205:1106–1116

Scalenghe R, Marsan FA (2009) The anthropogenic sealing of soils in urban areas. Landsc Urban Plan 90:1–10

Schaap MG, Bouten W (1997) Forest floor evaporation in a dense Douglas fir stand. J Hydrol 193:97–113

Schuepp PH (1972) Studies of forced-convection heat and mass transfer of fluttering realistic leaf models. Boundary-Layer Meteorol 2:263–274

Schuepp PH (1980) Heat and moisture transfer from flat surfaces in intermittent flow: a laboratory study. Agric Meteorol 22(2–4):351–366

Sharples S (1984) Full-scale measurements of convective energy losses from exterior building surfaces. Build Environ 19:31–39

Shibuya T, Tsuruyama J, Kitaya Y, Kiyota M (2006) Enhancement of photosynthesis and growth of tomato seedlings by forced ventilation within the canopy. Sci Hortic 109:218–222

Sucksdorff Y, Ottle C (1990) Application of satellite remote sensing to estimate areal evapotranspiration over a watershed. J Hydrol 121:321–333

Swanson R, Whitfield D (1981) A numerical analysis of heat pulse velocity theory and practice. J Exp Bot 32:221–239

Tang R, Li Z, Chen K, Jia Y, Ji C, Sun X (2013) Spatial-scale effect on the SEBAL model for evapotranspiration estimation using remote sensing data. Agric For Meteorol 174–175:28–42

Tanner CB (1963) Plant temperatures. Agron J 55:210–211

Thrope MR, Butler DR (1977) Heat transfer coefficients for leaves on orchard apple trees. Boundary-Layer Meteorol 12(1):61–73

Timmermans WJ, Kustas WP, Anderson MC, French AN (2007) An intercomparison of the surface energy balance algorithm for land (SEBAL) and the two-source energy balance (TSEB) modeling schemes. Remote Sens Environ 108:369–384

Verma SB, Baldocchi DD, Anderson DE, Matt DR, Clement RJ (1986) Eddy fluxes of CO_2, water vapor, and sensible heat over a deciduous forest. Boundary-Layer Meteorol 36:71–91

Vining RC, Blad BL (1992) Estimation of Sensible heat flux from remotely sensed canopy temperatures. J Geophys Res 97:18951–18954

Wilson KB, Baldocchi DD (2000) Seasonal and interannual variability of energy fluxes over a broad leaved temperate deciduous forest in North America. Agric For Meteorol 100:1–18

Wilson KB et al (2002a) Energy partitioning between latent and sensible heat flux during the warm season at FLUXNET sites. Water Resour Res 38:1294. https://doi.org/10.1029/2001WR000989

Wilson KB et al (2002b) Energy balance closure at FLUXNET sites. Agric For Meteorol 113:223–243

Yang R, Friedl MA (2003) Modeling the effects of three-dimensional vegetation structure on surface radiation and energy balance in boreal forests. J Geophys Res 108:8615. https://doi.org/10.1029/2002JD003109

Yang J, Zhang Y (2011) Water infiltration in urban soils and its effects on the quantity and quality of runoff. J Soil Sediment 11:751–761

Zhan X, Kustas WP, Humes KS (1996) An intercomparison study on models of sensible het flux over partial canopy surfaces with remotely sensed surface temperature. Remote Sens Environ 58:242–256

Publisher's Note Springer Nature remains neutral with regard to jurisdictional claims in published maps and institutional affiliations.